

## Optically pumped InAs quantum dot microdisk lasers

H. Cao,<sup>a)</sup> J. Y. Xu, and W. H. Xiang<sup>b)</sup>

*Department of Physics and Astronomy, Northwestern University, Evanston, Illinois 60208-3112*

Y. Ma, S.-H. Chang, and S. T. Ho

*Department of Electrical and Computer Engineering, Northwestern University, Evanston, Illinois 60208-3118*

G. S. Solomon

*Department of Electrical Engineering, Stanford University, Stanford, California 94305*

(Received 29 December 1999; accepted for publication 19 April 2000)

We have achieved lasing in InAs quantum dot embedded GaAs microdisks under optical pumping. Above the lasing threshold, a drastic increase of emission intensity is accompanied by a decrease of the spectral linewidth of the whispering gallery modes. The laser light is linearly polarized. The polarization direction is parallel to the disk plane. The wide gain spectrum of quantum dots allows simultaneous lasing in several whispering gallery modes of a microdisk. © 2000 American Institute of Physics. [S0003-6951(00)02824-2]

Optoelectronic devices based on highly confined photons and electrons are of interest for future low power, high speed application. Recently, there have been many advances in the fabrication of both semiconductor quantum dots and semiconductor microcavities. Using a self-organized growth technique made possible with the highly strained system, InGaAs quantum dots are formed and exhibit three-dimensional confinement of electrons. Semiconductor lasers with quantum dots as active media have been demonstrated.<sup>1-6</sup> On the other hand, high- $Q$  semiconductor microcavities are fabricated and provide strong optical confinement. By modifying the electromagnetic field distribution, microcavities can significantly enhance the spontaneous emission efficiency and reduce the lasing threshold. Recently, enhanced spontaneous emission of InAs quantum dots in GaAs/AlAs micropillars have been observed.<sup>7,8</sup> Moreover, quantum dot vertical-cavity surface-emitting lasers have also been demonstrated.<sup>9,10</sup> As compared to Fabry-Pérot cavities, microdisk cavities exhibit higher  $Q$  (up to 12 000), leading to larger enhancement of the spontaneous emission rate.<sup>11</sup> Microdisk lasers with quantum wells as active media have been fabricated, and very low lasing threshold has been achieved.<sup>12-17</sup> In this letter, we report lasing in quantum dot embedded microdisk cavities.

The quantum dot sample is grown by molecular beam epitaxy. The structure consists of a GaAs buffer layer, 500 nm  $\text{Al}_{0.7}\text{Ga}_{0.3}\text{As}$ , 45 nm GaAs, 2 monolayer (ML) InAs quantum dots, and 45 nm GaAs. The photoluminescence spectrum of quantum dots at 77 K is centered around 970 nm with a full width at half maximum (FWHM) of 20 nm.

The microdisks are fabricated by electron beam lithography and two steps of wet etch. 100 nm silicon dioxide ( $\text{SiO}_2$ ) is deposited on the wafer and used as the etch mask. Disk patterns are defined by electron beam lithography with

negative resist. The pattern is transferred from the  $e$ -beam resist to the  $\text{SiO}_2$  etch mask by reactive ion etch. It is followed by two steps of wet etch. The first step is a nonselective etch, i.e., the sample is unselectively etched down to the GaAs buffer layer in a dilute water solution of phosphoric acid ( $\text{H}_3\text{PO}_4$ ) and hydrodioxide ( $\text{H}_2\text{O}_2$ ). The etch rate is low enough to allow a good control of etch depth. The second step is a selective etch. A dilute solution of hydrofluoric acid is used to etch the  $\text{Al}_{0.7}\text{Ga}_{0.3}\text{As}$  layer without attacking GaAs layers and InAs quantum dots. With careful control of the etch time, microdisk structures are formed on top of pedestals. Figure 1 is the scanning electron micrograph of a microdisk structure. The edge of the microdisk is quite smooth.

The quantum dot microdisk is optically excited by a cw HeNe laser ( $\lambda = 633$  nm). The pump beam is focused by a microscope objective onto a single microdisk. The sample is mounted in a liquid nitrogen cryostat. The sample temperature can be continuously varied from 77 to 300 K. The pump beam is incident normally onto the microdisk through the front window of the cryostat. To efficiently collect the far-field emission from the whispering gallery modes, a lens is placed next to the side window of the cryostat to collect the emission from the side of the microdisk. A bandpass filter is used to block the scattered pump light. The emission spectrum is measured by a 0.5 m spectrometer with a cooled

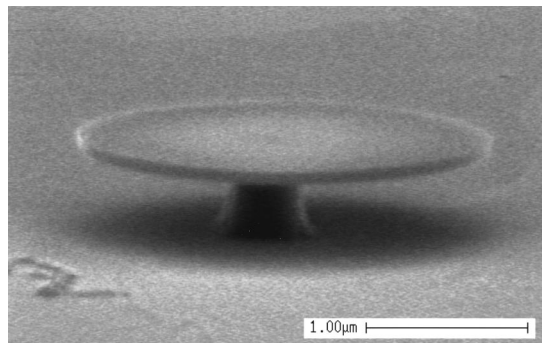


FIG. 1. Scanning electron micrograph of a microdisk

<sup>a)</sup>Author to whom correspondence should be addressed; electronic mail: h-cao@nwu.edu

<sup>b)</sup>On leave from College of Precision Instrument and Optoelectronics, Tianjin University, Tianjin 300072, China.

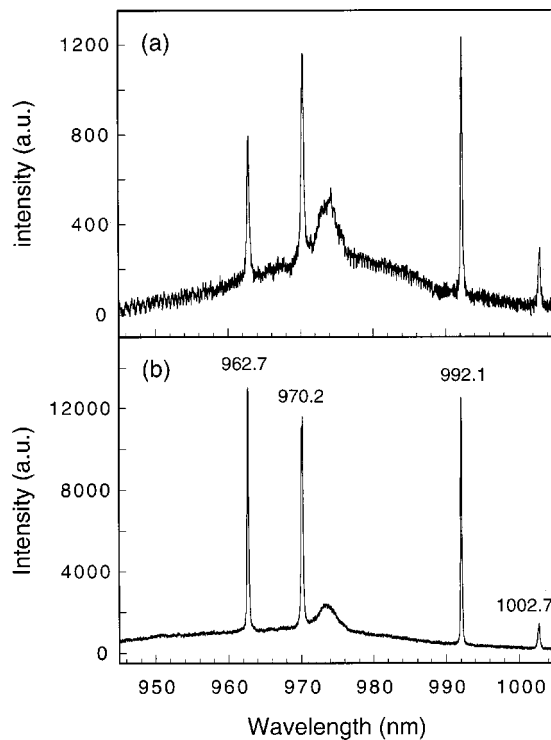


FIG. 2. Spectra of emission from the side of a  $3 \mu\text{m}$  disk when the incident pump power is (a)  $5 \mu\text{W}$  and (b)  $26 \mu\text{W}$ .

charge coupled device array detector. The spectral resolution is about  $1.7 \text{ \AA}$ .

Figure 2 shows the measured emission spectra at different pump powers. The diameter of the disk is  $3 \mu\text{m}$ . The sample temperature is  $77 \text{ K}$ . In the wavelength range of  $945\text{--}1005 \text{ nm}$ , we observe four sharp emission peaks. Their wavelengths are  $962.7$ ,  $970.2$ ,  $992.1$ , and  $1002.7 \text{ nm}$ , respectively. As the pump power increases, the four emission peaks become narrower, and their peak intensity increases drastically. Figure 3 plots the integrated emission intensity as a function of the incident pump power. A threshold behavior is clearly seen. When the incident pump power exceeds  $20 \mu\text{W}$ , the emission intensity increases much more rapidly with the pump power. Figure 4 plots the spectral linewidth of the emission peak at  $962.7 \text{ nm}$  as a function of the incident pump power. When the pump power is  $3.5 \mu\text{W}$ , the width of

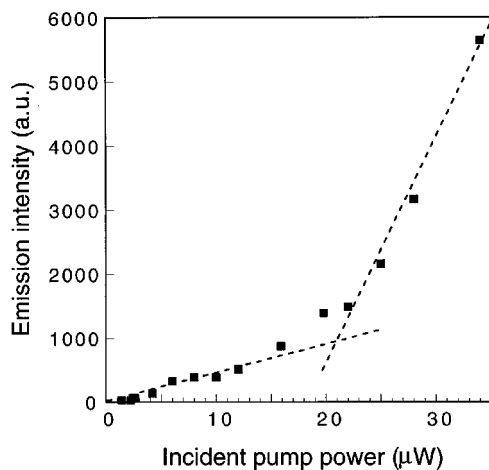


FIG. 3. The integrated emission intensity as a function of incident pump power.

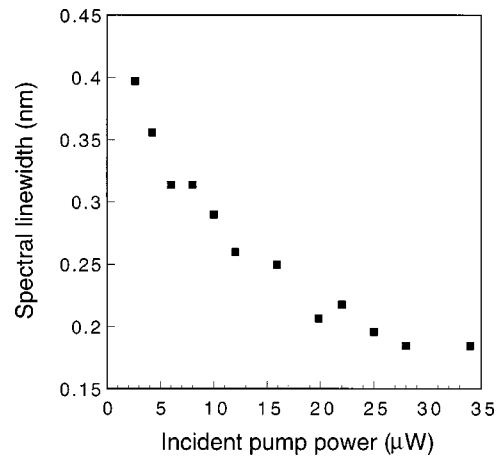


FIG. 4. The FWHM of the emission peak at  $962.7 \text{ nm}$  vs the incident pump power.

the emission peak is  $0.4 \text{ nm}$ . As the pump power increases, the emission linewidth decreases. At a pump power of  $29 \mu\text{W}$ , the spectral linewidth is reduced to  $0.18 \text{ nm}$ . The decrease of the spectral linewidth corresponds to an increase of temporal coherence. Therefore, Figs. 2–4 illustrate that lasing oscillation occurs in the quantum dot microdisk.

We calculate the whispering gallery modes of the microdisk. When we design the sample structure, we choose the thickness of the disk layer to be  $90 \text{ nm}$  so that it supports only the lowest order transverse electric (TE) mode. All transverse magnetic (TM) modes and higher order TE modes are suppressed. For the TE mode, the electrical field is parallel to the disk plane; while for the TM mode, the electrical field is perpendicular to the disk plane. We calculate the spatial profile of the TE guided wave in the disk layer. The lowest order TE mode has a spatial width of  $140 \text{ nm}$  in the direction perpendicular to the disk plane. Hence, part of the wave function of the lowest order TE mode is extended into the air. From the guided mode profile, we calculate the effective index of refraction  $n_{\text{eff}} \approx 2.53$ . Using the effective index of refraction, we find the frequencies of the whispering-gallery modes of the microdisk structure. The radial variation of the mode field is given by the  $m$ th order Bessel function  $J_m(2\pi r n_{\text{eff}}/\lambda_m)$ , where  $r$  is the radial coordinate, and  $m$  is the azimuthal number.  $J_m(2\pi r n_{\text{eff}}/\lambda_m)$  is zero when  $r$  is equal to the disk radius. By solving for the zero points of  $J_m$ , we obtain the wavelength  $\lambda_m$  of the whispering gallery modes. The order of the zero points for  $J_m$  gives the radial number  $n$ . For a fixed azimuthal number  $m$ , a smaller zero point, i.e., a zero point with smaller  $n$ , corresponds to a whispering gallery mode of a larger effective radius. Therefore, a whispering gallery mode is represented by  $\text{TE}_{m,n}$ . We identify the four lasing modes at  $962.7$ ,  $970.2$ ,  $992.1$ , and  $1002.7 \text{ nm}$  are  $\text{TE}_{19,1}$ ,  $\text{TE}_{15,2}$ ,  $\text{TE}_{18,1}$ , and  $\text{TE}_{14,2}$ , respectively.

To confirm our calculation, we have measured the polarization of the laser light from the side of the disk. Figure 5 shows the intensity of the lasing mode at  $962.7 \text{ nm}$  as a function of the polarization angle. We can see that the laser light is TE polarized, i.e., the polarization direction is parallel to the disk plane. Similar measurement shows that the other three modes at  $970.2$ ,  $992.1$ , and  $1002.7 \text{ nm}$  are also TE polarized.

Next, we increase the sample temperature. We have

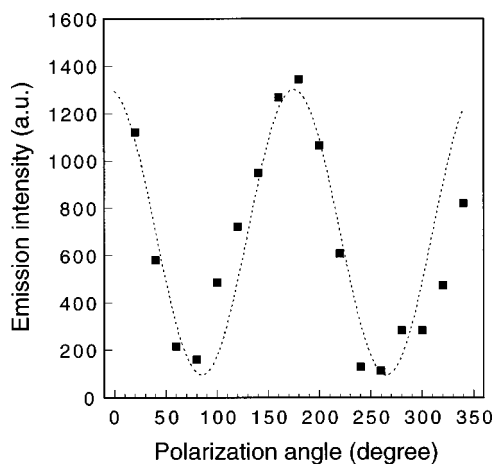


FIG. 5. Intensity of the lasing mode at 962.7 nm as a function of polarization angle. The emission is collected from the side of the microdisk. The intensity maximum corresponds to the polarization direction parallel to the disk plane. The incident pump power is 23  $\mu\text{W}$ .

achieved lasing in the 3  $\mu\text{m}$  microdisk when the sample temperature is 140 K. The incident pump power at the lasing threshold is about 40  $\mu\text{W}$ .

Finally, we compare quantum dot microdisk lasers with quantum well microdisk lasers. For a 3  $\mu\text{m}$  GaAs quantum well microdisk laser, lasing usually occurs in just one whispering gallery mode. This is because the width of the quantum well gain spectrum is less than the frequency spacing of the whispering gallery modes. However, the much broader gain spectrum of quantum dots allows simultaneous lasing in several whispering gallery modes of a 3  $\mu\text{m}$  microdisk. Another advantage of the quantum dot microdisk lasers is that they are free from surface recombination. One serious problem for quantum well microdisk lasers is that the surface states at the edge of the disk can reduce the lasing gain. Especially for GaAs quantum well microdisk lasers, surface passivation is necessary to achieve lasing.<sup>18</sup> The lasing threshold of quantum dot microdisk lasers is not much lower than the quantum well microdisk lasers due to the large inhomogeneous broadening of quantum dot energy levels.

In conclusion, we have achieved lasing in InAs quantum

dot embedded GaAs microdisks. Above the lasing threshold, a drastic increase of emission intensity is accompanied by a decrease of the spectral linewidth of the whispering gallery modes. The laser light is TE polarized. The wide gain spectrum of quantum dots allows simultaneous lasing in several whispering gallery modes of a microdisk.

This work is supported by the National Science Foundation under Grant No. ECS-9800068.

- <sup>1</sup>N. Kirkstaedter, N. Ledentsov, M. Grundmann, D. Bimberg, V. Ustinov, S. Ruvimov, M. Maximov, P. Kop'ev, and Zh. Alferov, *Electron. Lett.* **30**, 1416 (1994).
- <sup>2</sup>M. Grundmann, J. Christen, N. N. Ledentsov, J. Bohrer, D. Bimberg, S. S. Ruvimov, P. Werner, U. Richter, U. Gosele, J. Heydenreich, V. M. Ustinov, A. Yu. Egorov, A. E. Zhukov, P. S. Kop'ev, and Zh. I. Aferov, *Phys. Rev. Lett.* **74**, 4043 (1995).
- <sup>3</sup>K. Kamath, P. Bhattacharya, T. Sosnowski, T. Norris, and J. Philips, *Electron. Lett.* **32**, 1374 (1996).
- <sup>4</sup>H. Shoji, Y. Nakata, K. Mukai, Y. Sugiyama, M. Suagawara, N. Yokoyama, and H. Ishikawa, *Electron. Lett.* **32**, 2023 (1996).
- <sup>5</sup>R. Mirin, A. Gossard, and J. Bowers, *Electron. Lett.* **32**, 1732 (1996).
- <sup>6</sup>S. Fafard, K. Hinzer, S. Raymond, M. Dion, J. McCaffrey, Y. Feng, and S. Charbonneau, *Science* **274**, 1350 (1996).
- <sup>7</sup>J. M. Gerard, B. Sermage, B. Gayral, B. Legrand, E. Costard, and V. Thierry-Mieg, *Phys. Rev. Lett.* **81**, 1110 (1998).
- <sup>8</sup>L. A. Graham, D. L. Huffaker, and D. G. Deppe, *Appl. Phys. Lett.* **74**, 2408 (1999).
- <sup>9</sup>H. Saito, K. Nishi, I. Ogura, S. Sugov, and Y. Sugimoto, *Appl. Phys. Lett.* **69**, 3140 (1996).
- <sup>10</sup>D. L. Huffaker, O. Baklenov, L. A. Graham, B. G. Streetman, and D. G. Deppe, *Appl. Phys. Lett.* **70**, 2356 (1997).
- <sup>11</sup>B. Gayral, J. M. Gerard, A. Lemaitre, C. Dupuis, L. Manin, and J. L. Pelouard, *Appl. Phys. Lett.* **75**, 1908 (1999).
- <sup>12</sup>S. L. McCall, A. F. J. Levi, R. E. Slusher, S. J. Pearton, and R. A. Logan, *Appl. Phys. Lett.* **60**, 289 (1992).
- <sup>13</sup>A. F. J. Levi, R. E. Slusher, S. L. McCall, T. Tanbun-Ek, D. L. Coblentz, and S. J. Pearton, *Electron. Lett.* **28**, 1010 (1992).
- <sup>14</sup>A. F. J. Levi, S. L. McCall, S. J. Pearton, and R. A. Logan, *Electron. Lett.* **29**, 1666 (1993).
- <sup>15</sup>A. F. J. Levi, R. E. Slusher, S. L. McCall, S. J. Pearton, and W. S. Hobson, *Appl. Phys. Lett.* **62**, 2021 (1993).
- <sup>16</sup>R. E. Slusher, A. F. J. Levi, U. Mohideen, S. L. McCall, S. J. Pearton, and R. A. Logan, *Appl. Phys. Lett.* **63**, 1310 (1993).
- <sup>17</sup>T. Baba, M. Fujita, A. Sakai, M. Kihara, and R. Watanabe, *IEEE Photonics Technol. Lett.* **9**, 878 (1997).
- <sup>18</sup>U. Mohideen, W. S. Hobson, S. J. Pearton, F. Ren, and R. E. Slusher, *Appl. Phys. Lett.* **64**, 1911 (1994).